Reorientational Motions of Permethylated Cyclopentadienyl Rings in Polycrystalline Organometallic Compounds

Silvio Aime,*[1a] Dario Braga,*[1b] Lucia Cordero,[1a] Roberto Gobetto,[1a] Fabrizia Grepioni,[1b] Sandra Righi,[1b] and Silvana Sostero[1c]

Dipartimento di Chimica Inorganica, Chimica Fisica e Chimica dei Materiali, University of Torino, Via P. Giuria 7, 10125 Torino, Italy, Dipartimento di Chimica "G. Ciamician", University of Bologna, Via F. Selmi 2, 40126 Bologna, Italy, and Centro Fotochimica del CNR, c/o Dipartimento di Chimica, University of Ferrara, Via Borsari 46, 44100 Ferrara, Italy

Received January 2, 1992

The dynamic behavior in the solid state of $(C_5Me_5)_2Fe$ (I), $(C_5Me_5)Rh(CO)_2$ (II), $(C_5Me_5)_2Cr_2(CO)_4$ (III), $(C_5Me_5)Fe_2(\mu_2\text{-}CO)_2(CO)_2$ (IV), and $(C_5Me_5)_2Rh_2(\mu_2\text{-}Cl)_2Cl_2$ (V) has been investigated by variable-temperature ^1H spin–lattice relaxation time measurements and potential energy barrier calculations within the pairwise atom–atom approach. In all the cases two different processes have been detected corresponding to the rotation of the methyl group about its C_3 axis and to the reorientation of the cyclopentadienyl ligand about its C_5 axis, respectively. The separate intramolecular and intermolecular contributions to the total reorientational barriers have been evaluated. It has been shown that in crystalline III and IV a synchronous motion of the methyl groups during ring reorientation reduces intramolecular repulsions between the H atoms of the methyl groups and the CO ligands and affords a low-energy reorientational path. ^{13}C spin–lattice relaxation times have also been determined for the individual carbon atoms by using Torchia's pulse sequence. The ^{13}C-T_1 values observed for ring carbons have been rationalized on the basis of two relaxation interactions (dipole–dipole and chemical shift anisotropy) modulated by the motions involving the permethylated cyclopentadienyl rings. The chemical shift anisotropies of cyclopentadienyl ^{13}C resonances have been determined on chloroform solutions of compounds II–V at different magnetic field strengths. A qualitative comparison between solution- and solid-state ^{13}C relaxation data shows that the same relaxation mechanisms are operative in both physical states.

NMR spectroscopy is a powerful tool for the investigation of dynamic processes occurring in the solid state.[2] Low-resolution "wide-line" and high-resolution "magic-angle" spinning techniques have been used to determine the activation energy for the reorientation of a variety of π-bonded ligands in organometallic molecules.[3] The potential energy barriers associated with reorientational processes of rigid molecular fragments have also been evaluated by means of the pairwise atom–atom potential energy method[4] by using the information in the crystal structure as determined by diffraction methods. The combined use of spectroscopic and crystallographic methods to investigate dynamic phenomena occurring in crystalline organometallic materials has been recently reviewed.[5]

In preceding papers[6] we investigated the relationship between the rotation of cyclopentadienyl rings and the proton and ^{13}C-relaxation rates[6a] and that between barrier height and extent of ring motion about equilibrium positions as revealed by the atomic anisotropic displacement parameters[6b] in crystals of the cis and trans isomers of $(C_5H_5)_2Fe_2(CO)_4$. More recently, these methods have been jointly applied to study the dynamic behavior in crystals of methyl-substituted $(\eta^6\text{-arene})M(CO)_3$ complexes.[7]

In this paper we now extend this approach to the neutral mono- and dinuclear organometallic complexes $(C_5Me_5)_2Fe$ (I), $(C_5Me_5)Rh(CO)_2$ (II), $(C_5Me_5)_2Cr_2(CO)_4$ (III), $(C_5Me_5)Fe_2(\mu_2\text{-}CO)_2(CO)_2$ (IV), and $(C_5Me_5)_2Rh_2(\mu_2\text{-}Cl)_2Cl_2$ (V). The molecular structures of these species are sketched in Figure 1. They are characterized by the presence of permethylated cyclopentadienyl ligands. These ligands display two distinct motions in the solid state, namely reorientation of the methyl groups around their C_3 axes and reorientation of each cyclopentadienyl ligand as a whole around its C_5 axis. The aim of this study is to understand the relationship between solid-state ^1H and ^{13}C relaxation behavior in the presence of molecular motions and to gain insights into the intramolecular and intermolecular contributions to the reorientational barriers involving substituted cyclopentadienyl rings.

Results and Discussion

Wide-Line ^1H-T_1 Experiments. The values of proton spin–lattice relaxation times (T_1) measured as a function of temperature for all species discussed herein are plotted as log T_1 versus $10^3/T$ (K) in Figure 2. In the presence of two kinds of motion, the variation of proton T_1 with temperature should exhibit two minima (at $\omega_H\tau_c = 0.62$), one corresponding to the reorientation of the CH_3 group as a triangular rotor and one arising from the rotation of the cyclopentadienyl ring about its coordination axis.

The temperature range accessible in our experiments (373–153 K) did not allow us to sweep the entire T_1 profiles. Nevertheless, two well-defined and distinct processes can be easily observed for I, II, IV, and V (Figure 2a,b,d,e). For III (Figure 2c) we were unable to observe the T_1 maximum and the corre-

(1) (a) University of Torino. (b) University of Bologna. (c) University of Ferrara.
(2) (a) Fyfe, C. A. *Solid State NMR for Chemists*; CFC Press: Guelph, Canada, 1984. (b) Mehring, M. *Principles of High Resolution NMR in Solids*; Springer-Verlag: Berlin, 1983. (c) Fyfe, C. A. *Molecular Complexes*, Foster, R., Ed.; Logos Press: London, 1973; Vol. VI, p 209. (d) Weiss, A. *Angew. Chem., Int. Ed. Engl.* **1972**, *11*, 607. (e) Goncalves, A. M. P. *Prog. Solid State Chem.* **1980**, *13*, 1. (f) Allen, P. S. *International Review of Science-Physical Chemistry Series One*; Buckingham, A. O., Ed.; Butterworth: London, 1972; Vol. 4, p 43.
(3) (a) Fyfe, C. A. *J. Am. Chem. Soc.* **1972**, *94*, 2690. (b) Gilson, D. F. R.; Gomez, G. *J. Org. Chem.* **1982**, *240*, 41. (c) Harvey, P. D.; Butler, I. S.; Gilson, D. F. R. *Inorg. Chem.* **1986**, *25*, 1009. (d) Heyers, S. J.; Dobson, C. M. *Inorg. Chem.* **1991**, *113*, 463.
(4) (a) Pertsin, A. J.; Kitaigorodsky, A. I. *The Atom-Atom Potential Method*; Springer-Verlag: Berlin, 1987. (b) Kitaigorodsky, A. I. *Chem. Soc. Rev.* **1978**, *7*, 133.
(5) Braga, D. *Chem. Rev.*, in press.
(6) (a) Aime, S.; Botta, M.; Gobetto, R.; Orlandi, A. *Magn. Reson. Chem.* **1990**, *28*, 552. (b) Braga, D.; Gradella, C.; Grepioni, F. *J. Chem. Soc., Dalton Trans.* **1989**, 1721.
(7) Aime, S.; Braga, D.; Gobetto, R.; Grepioni, F.; Orlandi, A. *Inorg. Chem.* **1991**, *30*, 951.

0020-1669/92/1331-3054$03.00/0

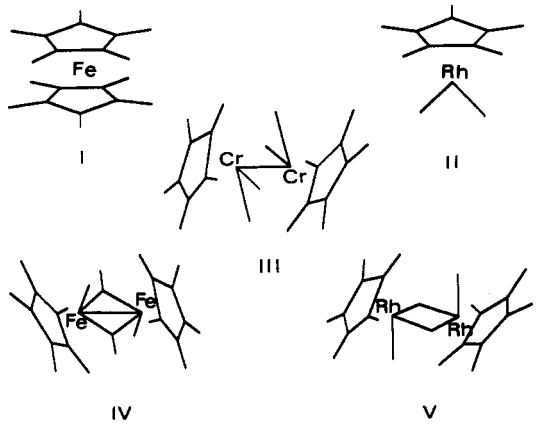

Figure 1. Schematic representation of the structures of $(C_5Me_5)_2Fe$ (I), $(C_5Me_5)Rh(CO)_2$ (II), $(C_5Me_5)_2Cr_2(CO)_4$ (III), $(C_5Me_5)Fe_2(\mu_2\text{-}CO)_2(CO)_2$ (IV), and $(C_5Me_5)_2Rh_2(\mu_2\text{-}Cl)_2Cl_2$ (V).

sponding low-temperature methyl reorientation regime. However, the significant asymmetry of the curve with respect to the minimum is indicative of the concomitant contribution of two motions to the observed relaxation rates in the low-temperature region.

We analyzed the data using the known expression (eq 1) of Kubo and Tomita[8] assuming that each correlation time $\tau_{c(i)}$ follows

$$1/T_1 = \sum_i C_i[\tau_{c(i)}(1 + \omega^2\tau_{c(i)})^{-1} + 4\tau_c(1 + 4\omega^2\tau_{c(i)}^2)^{-1}] \quad (1)$$

the simple Arrhenius-type activation law $\tau_{c(i)} = \tau_{0(i)} \exp[E_a(i)/RT]$. The slope of the curve of log T_1 vs $10^3/T$ affords the activation energy (E_a) associated with the dynamic process which is more efficient toward proton relaxation in a given temperature range. Furthermore, the observation of a T_1 minimum allows a direct determination of C and τ_c values. Table I summarizes the values found from the best-fit procedure for E_a, C, and τ_c parameters for ring rotation and E_a for methyl reorientation. As expected, the comparison between the calculated and the observed profiles shows large differences in the intermediate region of long T_1's between the two wells as a consequence of the concomitance of two nonindependent dynamic processes.

The T_1 profile of I has been measured at 270 and 60 MHz, respectively (Figure 2a), and the observed behavior is easily understood on the basis of eq 1: at high temperature, where $\omega_H\tau_c \ll 1$, T_1 is proportional to τ_c^{-1} and it is independent of the frequency, while at low temperature, where $\omega_H\tau_c \gg 1$, T_1 is proportional to $\omega_H^2\tau_c$. It follows that the T_1 values coincide at high temperature, and the minima in the two profiles differ by about 60 K.

The activation energies for CH_3 rotation fall in a quite narrow range (6.5–10.5 kJ·mol^{-1}); the relatively low values reflect the large distance between neighbor molecules. For comparison, in solid amino acids, Andrew and co-workers found E_a values for methyl reorientation ranging from 6.7 to 22 kJ·mol^{-1}.[9]

The activation energies for C_5Me_5 reorientation show significant differences that need to be analyzed in more detail. To do this we resort to the evaluation of the potential energy barriers associated with the various kinds of motion by means of the atom–atom potential energy method (see below). However, we may note that the thermally activated rotation of the C_5Me_5 groups appears to follow the simple empirical relationship $E_a/RT_{min} =$ 5.7 ± 1, where T_{min} is the temperature (K) at which the T_1 minimum occurs (see Figure 3).

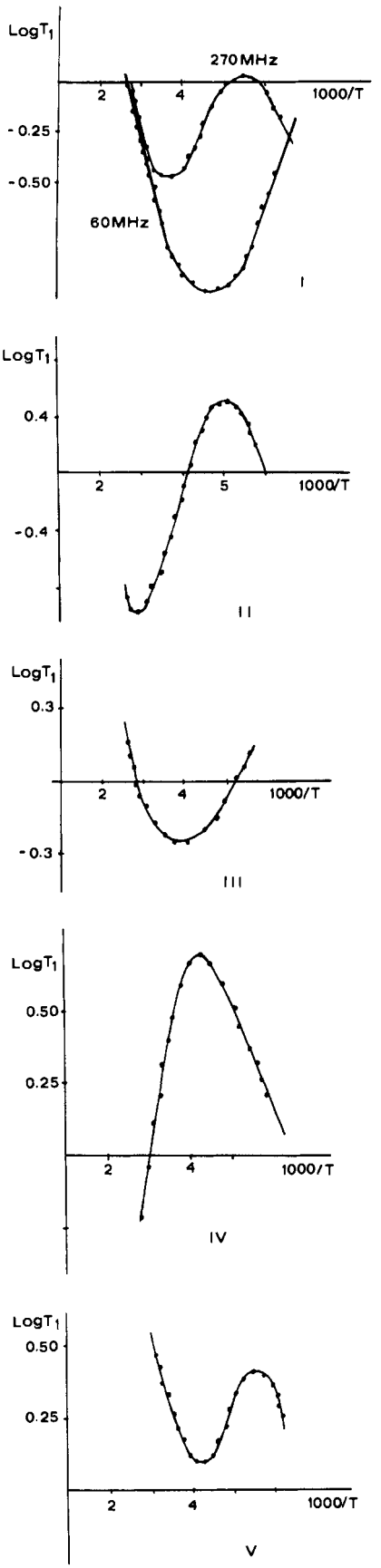

Figure 2. Variation of proton spin–lattice relaxation times T_1 with inverse temperature T^{-1} for crystalline I–V at 270 MHz (from top to bottom): (a) $(C_5Me_5)_2Fe$ (I) (measured also at 60 MHz); (b) $(C_5Me_5)Rh(CO)_2$ (II); (c) $(C_5Me_5)_2Cr_2(CO)_2$ (III); (d) $(C_5Me_5)Fe_2(\mu_2\text{-}CO)_2(CO)_2$ (IV); (e) $(C_5Me_5)_2Rh_2(\mu_2\text{-}Cl)_2Cl_2$ (V).

(8) Kubo, R.; Tomita, K. *J. Phys. Soc.* **1954**, *9*, 888.
(9) Andrew, E. R.; Hinshaw, W. S.; Hutchins, M. G.; Sjöblom, R. O.; Canepa, P. C. *Mol. Phys.* **1976**, *32*, 795.

Table I. Relaxation Parameters for Molecular Motion in Crystalline I–V and Comparison with the Results of Atom–Atom Potential Energy Barrier Calculations[a]

compd	τ_0^{Cp}	C^{Cp}	E_a^{Me}	E_a^{Cp}	PB_{tot}	PB_{intra}	PB_{inter}
$Fe(C_5Me_5)_2$	1.13	3.3	6.5	12.5	10.0	3.8	6.3
$Rh(C_5Me_5)(CO)_2$	1.14	3.7	10.5	22.0	15.9		15.9
$Cr_2(C_5Me_5)_2(CO)_4$	1.12	2.6		12.1	16.7	9.6	7.5
$Fe_2(C_5Me_5)_2(CO)_4$	0.97	7.7	6.7	24.0	25.1	18.3	7.9
$Rh_2(C_5Me_5)_2Cl_4$	1.96	0.9		10.1	15.0	1.6	13.8

[a] τ_0^{Cp}/s ($\times 10^{-12}$); C^{Cp}/s^{-2} ($\times 10^{-9}$); E_a, PB/kJ·mol^{-1}.

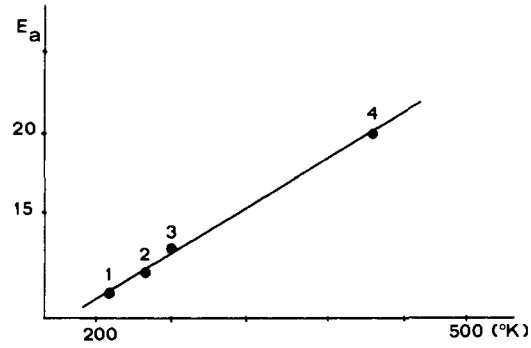

Figure 3. Plot of E_a versus T_{min} for (1) $(C_5Me_5)_2Fe$, (2) $(C_5Me_5)Rh(CO)_2$, (3) $(C_5Me_5)_2Cr_2(CO)_2$, and (4) $(C_5Me_5)_2Rh_2(\mu_2\text{-}Cl)_2Cl_2$.

Potential Energy Barrier Calculations. In previous papers[7,10] we have employed the atom–atom pairwise potential energy method[4] to estimate the potential energy barrier (PB) opposing the reorientational motion of molecular fragments in the solid state. The method allows a separate estimate of the *intramolecular* (PB_{intra}) and *intermolecular* (PB_{inter}) contributions to the total reorientational barrier (PB_{tot}).[11] This aspect is particularly relevant in discussing the results of the NMR experiments in which the two terms are not separated. The NMR activation energies are, in fact, obtained as mean values over a broad temperature range and convolute all *internal* (intramolecular bonding and nonbonding interactions) and *external* contributions (intermolecular interactions and correlated and uncorrelated motions) to the energy barrier. PB calculations are carried out within the "static environment" approximation, i.e. without cooperation or relaxation of the molecules surrounding the reorienting fragment.[12] The methyl groups are treated as chlorine atoms centered on the C(Me) positions to take into account methyl rotation during ring reorientation.[7] The values of PB_{intra}, PB_{inter}, and PB_{tot} for all the species discussed herein are reported in Table I and compared with the E_a values obtained as described above.

The distribution of the first-neighboring molecules around the reference one (those constituting the so-called "enclosure shell", ES[13]) is also easily accessible from atom–atom potential energy calculations.

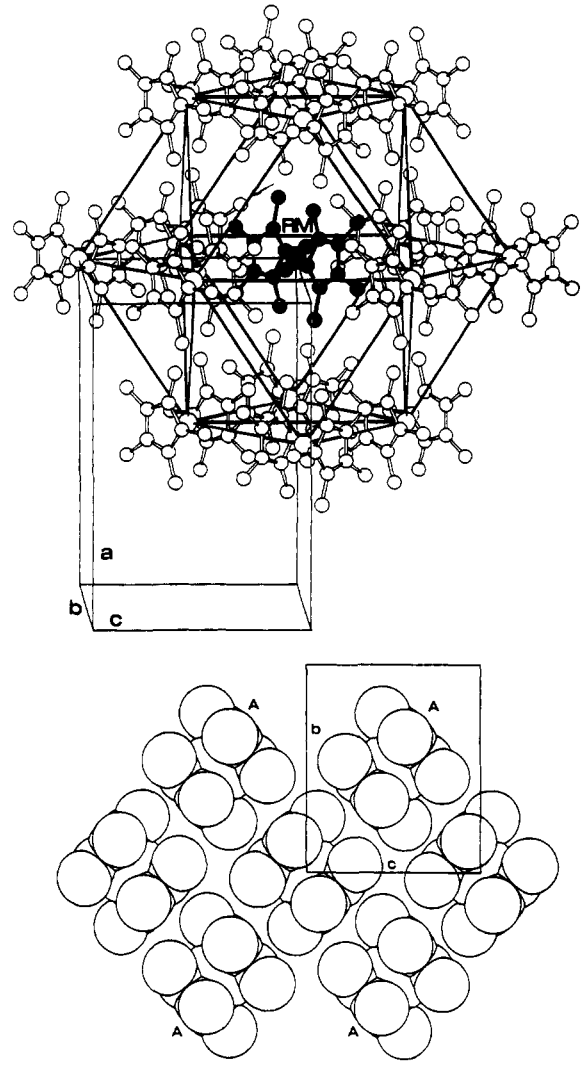

Figure 4. (a) Top: Distribution of the first-neighboring molecules in crystalline $(C_5Me_5)_2Fe$. H-atoms are omitted for clarity. The space filling outlines in (b, bottom) show the molecular distribution in the equatorial plane of the ES: the molecular axes are approximately at right angles to one another.

All calculations were carried out with the aid of the computer program OPEC.[14] SCHAKAL88[15] was used for the graphical representation of the results. Fractional atomic coordinates and crystallographic parameters for the species discussed herein were obtained from the Cambridge Crystallographic Data Base or from the original structural reports.[16-20]

Let us first examine the molecular distribution and reorientational motion in crystals of the mononuclear complexes I and II.

The ES of I[16] consists of 14 molecules (see Figure 4a) organized in layers stacked in *ABA* sequence. This molecular distribution closely resembles that observed in the monoclinic crystals of ferrocene and nickelocene.[21] As in these latter crystals, the molecules

(10) (a) Braga, D.; Grepioni, F. *Organometallics* **1991**, *10*, 1254. (b) Braga, D.; Grepioni, F. *Organometallics* **1991**, *10*, 2564. (c) Braga, D.; Grepioni, F.; Parisini, E. *Organometallics* **1991**, *10*, 3735.

(11) We calculate first the packing potential energy corresponding to the observed crystal structure (PPE_{obs}) by means of the expression: $PPE_{obs} = \sum_i\sum_j[A \exp(-Br_{ij}) - Cr_{ij}^{-6}]$, where r_{ij} represents a nonbonded atom–atom distance within the cutoff distance of 10 Å. PPE is then recalculated for various rotameric conformations (every 10° in this study) of the reorientating fragment affording PB = PPE – PPE_{obs}. The separate intra- and intermolecular contributions to PPE can be estimated. The values of the coefficients *A*, *B*, and *C* used in this work are taken from the following sources: Mirsky, K. *Computing in Crystallography, Proceedings of the International Summer School on Crystallographic Computing*; Delf University Press: Twente, The Netherlands, 1978; p 169. Gavezzotti, A.; Simonetta, M. *Chem. Rev.* **1982**, *82*, 1.

(12) Gavezzotti, A.; Simonetta, M. *Acta Crystallogr., Sect. A* **1976**, *32*, 997.

(13) The molecules forming the ES are selected among the large number of molecules generated by space group symmetry within the cutoff of 10 Å on the basis of their contribution to the PPE. See also: Braga, D.; Grepioni, F.; Sabatino, P. *J. Chem. Soc., Dalton Trans.* **1990**, 3137.

(14) Gavezzotti, A. OPEC. Organic Packing Potential Energy Calculations. University of Milano, Italy. See also: Gavezzotti, A. *J. Am. Chem. Soc.* **1983**, *195*, 5220.

(15) Keller, E. SCHAKAL88. Graphical Representation of Molecular Models. University of Freiburg, FRG.

(16) Freyberg, D. P.; Robbins, J. L.; Raymond, K. N.; Swart, J. C. *J. Am. Chem. Soc.* **1979**, *101*, 892.

(17) (a) Lichtenberger, D. L.; Blevins, C. H.; Ortega, R. B. *Organometallics* **1984**, *3*, 1614. (b) Braunstein, P.; Lehner, H.; Matt, D.; Tiripicchio, A.; Tiripicchio Camellini, M. *Nouv. J. Chim.* **1985**, *9*, 597.

(18) Teller, R. G.; Williams, J. M. *Inorg. Chem.* **1980**, *19*, 2770.

(19) Potenza, J.; Giordano, P.; Mastropaolo, D.; Efraty, A.; King, R. B. *J. Chem. Soc., Chem. Commun.* **1972**, 1333.

(20) Churchill, M. R.; Julis, S. A.; Rotella, F. J. *Inorg. Chem.* **1977**, *16*, 1137.

(21) Braga, D.; Grepioni, F. *Organometallics* **1992**, *11*, 711.

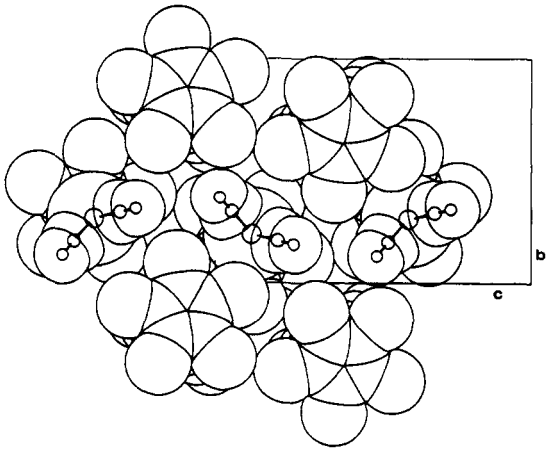

Figure 5. Space-filling representation of the ES molecules in crystalline $(C_5Me_5)Rh(CO)_2$ (II) showing how the $(CO)_2$ unit is tightly interlocked.

within the layers are approximately at right angles to one another (see Figure 4b). The intermolecular reorientational barrier in I is quite low (PB_{inter} = 6.3 kJ·mol^{-1}), even lower than in monoclinic ferrocene (8.4 and 9.2 kJ·mol^{-1} at 298 and 173 K, respectively).[21] The intramolecular term, which is negligible in ferrocene, is instead appreciable in I (PB_{intra} = 3.8 kJ·mol^{-1}). This value is in good agreement with the barrier to internal rotation estimated from gas-phase electron diffraction[22] (ca. 4 kJ·mol^{-1}) although it should be kept in mind that PB_{intra} contains information only of a nonbonding nature. Expectedly, both inter- and intramolecular profiles show minima every $2\pi/5$ rotational jumps. The two curves are "in phase" so that PB_{inter} and PB_{intra} sum up to give a total reorientational barrier PB_{tot} of 10.0 kJ·mol^{-1} (see also below).

The ES of II is also constituted of 14 first-neighboring molecules.[17] These molecules are not assembled in a highly regular coordination polyhedron as in I. This is due to the "irregular" molecular shape of II determined by the presence of a large and flat C_5Me_5 fragment possessing 5-fold symmetry and of a dicarbonyl unit possessing 2-fold symmetry. Each molecular layer in the lattice of II contains alternating zigzag rows of C_5Me_5 and dicarbonyl units. This arrangement closely resembles that previously found in crystals of $(C_6H_6)Cr(CO)_3$ and (C_6Me_6)-$Cr(CO)_3$.[10b] Inspection of the ligand interlocking in the lattice of II (see Figure 5) shows that, while reorientation of the dicarbonyl unit would lead to "clashes" of the O-atoms into the methyl groups of the neighboring molecules, reorientation of the discoidal C_5Me_5 ligand is almost unhindered. In agreement with this inference PB_{inter} for reorientation of the dicarbonyl unit is very large (>100 kJ·mol^{-1}), while PB_{inter} for C_5Me_5 $2\pi/5$ jumps is 15.9 kJ·mol^{-1}. The intramolecular contribution to the barrier is nil since the O-atoms are quite far away from the C_5Me_5 ligand. This behavior is in exact accord with that of related molecules such as $(C_6H_6)M(CO)_3$ and $(C_6Me_6)M(CO)_3$ (M = Cr, Mo).[10b]

While PB_{intra} is negligible in I and II, this is not so for the dinuclear species III and IV, where the motion of the C_5Me_5 ligands leads to "intramolecular clashes" between the H-atoms of the methyl groups and the CO ligands. For example, if the experimentally observed methyl group orientation[18] in IV is not changed during ring reorientation, some intramolecular H··CO separations become extremely short (shortest distances:[23] H··O = 2.04, H··C = 2.5 Å) giving rise to important repulsive interactions. This simple model, however, does not take into account methyl rotation *during* C_5Me_5 reorientation. The *simultaneous* motion of the two fragments can be studied by evaluating PB_{intra} for a complete rotation of one methyl group every 10° rotational step of the C_5 ring around its coordination axis (see Figure 6). As expected, there are large maxima (of the order of 100 kJ·mol^{-1}) corresponding to a complete methyl rotation *while* the group is kept eclipsed over the terminal CO. A low-energy path (broken line) is available for the motion of the two fragments if $-CH_3$ and C_5Me_5 rotations are synchronous, i.e. the methyl H-atoms "pass over" the CO group during ring reorientation, as shown in Figure 7. These observations, though based on a simplistic model, suggest that CH_3 rotation is not *independent from* the motion of the C_5Me_5 fragment; rather the two motions need to become *correlated* to make possible the reorientation of this latter ligand.

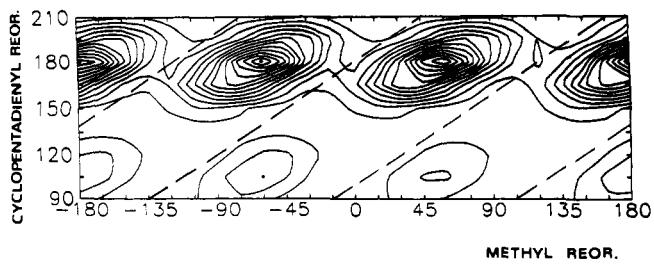

Figure 6. Tridimensional PB_{intra} plot for simultaneous methyl (abscissa) and cyclopentadienyl (ordinate) reorientation in the case of IV. The broken lines represent low-energy paths accessible to the ligand if methyl rotation accompanies cyclopentadienyl reorientation. Contour lines are drawn at 10 kJ·mol^{-1} steps, the minimum being set at 0 kJ·mol^{-1} for the original orientations of the two groups.

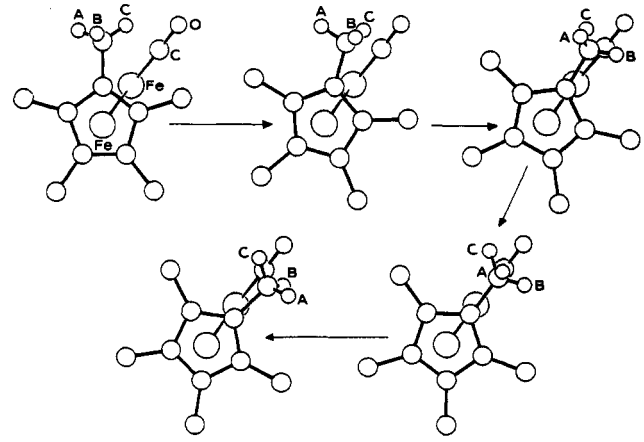

Figure 7. Schematic representation of the synchronous motion of the cyclopentadienyl ring and of one methyl group in the structure of IV. The methyl group "passes over" the terminal CO group bound to the opposite iron atom.

An analogous situation is observed in crystalline III, the main difference between III and IV arising from the different bonding of the four CO groups (two symmetric bridges and two terminal CO's in IV,[18] four "bent" terminal CO's in III[19]). As shown in Table I, the value of PB_{intra} is larger in IV than in III (18.3 versus 9.6 kJ·mol^{-1}), while the values of PB_{inter} are comparable in the two crystals (7.5 and 7.9 kJ·mol^{-1}, in III and IV, respectively). The total reorientational barriers PB_{tot} is 16.7 and 25.1 kJ·mol^{-1}, for III and IV, respectively, are in good agreement with the spectroscopic results.

The intramolecular contribution to ring reorientation in crystalline V[20] is much smaller than in III and IV [PB_{intra} = 1.6 kJ·mol^{-1}] and comparable to the value obtained for I. This is not surprising because the substitution of chlorine atoms for the CO's in III and IV and the lengthening of the intermetallic separation reduces drastically the intramolecular constraints to ring reorientation. The intermolecular barrier, on the other hand, is quite large (13.8 kJ·mol^{-1}) and comparable to that in II (15.9 kJ·mol^{-1}).

(22) Almenningen, A.; Haaland, A.; Samdal, S.; Brunvoll, J.; Robbins, J. L.; Smart, J. C. *J. Organomet. Chem.* **1979**, *173*, 293.

(23) In keeping with the basic assumption of the pairwise potential energy method, namely that the interatomic interactions depend on the distances between atomic nuclei, the H-atom positions were derived from those "observed" in the diffraction experiment (except for V) by sliding the H-centers along the C–H vectors to a distance of 1.08 Å.

Table II. Solid-State ^{13}C Chemical Shift and Spin–Lattice Relaxation Data Measured at 67.8 MHz at 298 K

compd	δ_{Me}/ppm	δ_{Cp}/ppm	T_1^{Me}/s	T_1^{Cp}/s
$Fe(C_5Me_5)_2$	10.79	79.2	1.9	8.7
$Rh(C_5Me_5)(CO)_2$	11.4	101.7	0.7	3.7
$Cr_2(C_5Me_5)_2(CO)_4$	10.6	100.5	1.7	6.0
$Fe_2(C_5Me_5)_2(CO)_4$	9.7	99.0	1.1	4.2
$Rh_2(C_5Me_5)_2Cl_4$	11.5	95.4	7.7	27.0

The overall barrier (15.0 kJ·mol^{-1}) is therefore determined mainly at the intermolecular level.

^{13}C CP-MAS NMR Experiments. The ^{13}C NMR spectra of I–V at room temperature recorded under CP-MAS conditions show a single peak for both methyl and cyclopentadienyl resonances (Table II) as found in solution. The lack of more resonances confirms the presence of a reorientational process which averages out the structural differences among the cyclopentadienyl carbon atoms. The relaxation time T_1 values measured through the use of Torchia's pulse sequence[24] for methyl and cyclopentadienyl carbon resonance are reported in Table II.

Except for V, the measured T_1's are of the same order of magnitude of the values commonly found in solution for these types of resonances (vide infra). This behavior would suggest that the processes operative in the solid state are similar to those active in solution (although in the solid state the correlation times are probably associated only with internal motions rather than with overall molecular tumbling as occurs in the liquid state). The most straightforward mechanism for relaxation is provided by the random reorientation of the methyl groups, which will modulate the dipolar interaction between the protons of the CH_3 groups and the methyl and cyclopentadienyl ^{13}C nuclei. However, the observed T_1 values for the ^{13}C cyclopentadienyl resonances appear shorter than expected on the basis of the occurrence of the dipolar mechanism alone [in this case theory would predict that $T_1(CH_3)/T_1(C\text{–}CH_3) = r_{C\text{–}H}^6/r_{C\text{–}CH_3}^6$].

In order to gain insights into the relaxation mechanism, we need to know which are the correlation times, τ_c, associated with the methyl rotation at ambient temperature. The corresponding τ_c^{Cp} for cyclopentadienyl rotation about its C_5 axis are known from the "wide-line" proton-T_1 values, which, at room temperature, are determined mainly by this type of motion.

It is well-known that the spin–lattice relaxation of a spectral line in a MAS spectrum is not described by a single exponential decay due to the distribution of all possible orientations with respect to the magnetic field. However, the relaxation dependence on the orientation relative to the H_0 field vanishes because of the very high reorientation rates of the methyl groups at ambient temperature. It has been suggested[25] that, under these conditions, the dipolar contribution to the longitudinal relaxation of methyl ^{13}C resonances can be evaluated by the simple relationship

$$1/T^1_{Me} = {}^4/_9[(\gamma_c^2\gamma_H^2\hbar^2)/r_{CH}^6]\tau_c^{Me} \qquad (2)$$

Assuming an average C··H distance of 1.08 Å, we can obtain the τ_c^{Me} values from the experimental T_1 data for the methyl ^{13}C resonances. Two main mechanisms are expected to be operative for the spin–lattice relaxation of the cyclopentadienyl carbons: (i) a dipolar interaction with the nearest methyl hydrogens; (ii) a chemical shift anisotropy due to rapid reorientation of the cyclopentadienyl ring. By considering that in the permethylated compounds the averaged C(ring)··H(methyl) separation is 2.16 Å for the C–CH_3 group and the angle between the C··H vector and the rotation axis in the methyl group is 29.8°, we may conveniently evaluate the dipolar contribution from the methyl protons to the cyclopentadienyl carbonyl by using eq 3,[26] where

$$1/T_1^{DD} = {}^1/_{16}\gamma_C^2\gamma_H^2\hbar^2 J_0(\omega_H - \omega_C) + 18J_1(\omega_C) + 9J_2(\omega_H - \omega_C) \qquad (3)$$

$$J_m(\omega) = k_M\sum_i r_{CHi}^{-6}N_i({}^3/_4)(\sin^2 2\beta_i + \sin^4\beta_i)(2\tau_{ci}/(1+\omega^2\tau_{ci}^2))$$

$K_0 = {}^4/_5$, $K_1 = {}^2/_{15}$, $K_2 = {}^8/_{15}$, β_i is the angle between the C–H vector and the rotation axis in the methyl group, N_i is the number of equivalent protons in the ith group, and τ_c refers to the methyl reorientation. Once $1/T_1^{DD}$ has been calculated through this procedure, the evaluation of the term $1/T_1^{CSA}$ is possible via eqs 4 and 5, where $\Delta\sigma$ is the chemical shift anisotropy of the cyclopentadienyl resonance.

$$1/T_1^{Cp} = 1/T_1^{DD} + 1/T_1^{CSA} \qquad (4)$$

$$1/T_1^{CSA} = {}^2/_{15}\gamma_c^2B_0^2\Delta\sigma^2\tau_c^{Cp} \qquad (5)$$

We estimate the contribution due to the CSA mechanism by making use of $\Delta\sigma$ values obtained from other sources. In the literature, this parameter is available only for I. For all other species $\Delta\sigma$ was evaluated by measuring the ^{13}C spin–lattice relaxation times in $CDCl_3$ solution at two magnetic field strengths. The computed $1/T_1^{CSA}$ term was then added to the dipolar contribution; the values of the resulting T_1's are reported in Table III together with the relevant parameters employed in the calculations. The agreement between theoretical and experimental values appears to be quite satisfactory if one takes into account the following: (i) The methyl groups are assumed to relax only by the dipolar mechanism, thus neglecting spin-rotation and chemical shift anisotropy contributions. (ii) The dipolar contribution to the cyclopentadienyl carbon relaxation due to the methyl groups not directly bonded is also neglected in the calculation; to take this contribution into account a much more complicated equation should be used since the carbon atom does not lie on the methyl reorientation axis. (iii) τ_c^{Me} values are extracted from the T_1^{Me} values without further discriminating between the concomitant rotation of the methyl group about its C_3 axis and the reorientation of the C_5Me_5 group around its C_5 axis.

The need to have an independent route for the evaluation of $\Delta\sigma$ for crystalline derivatives led us to measure the solution ^{13}C spin–lattice relaxation times T_1 and NOE's of cyclopentadienyl resonances at 6.3 and 9.4 T (see Table IV). The usual workup

Table III. Observed and Calculated Values of the ^{13}C Spin–Lattice Relaxation Times for I–V and Relevant Parameters Used in the Calculations

compd	τ_{Me}/s	τ_{Cp}/s	$\Delta\sigma_{Cp}$/ppm	T_1^{Cp}-(exp)/s	T_1^{Cp}-(calc)/s
$Fe(C_5Me_5)_2$	5.7×10^{-11}	2.0×10^{-10}	83.4	8.7	15.7
$Rh(C_5Me_5)(CO)_2$	1.6×10^{-10}	8.1×10^{-9}	131.0	3.6	2.8
$Cr_2(C_5Me_5)_2(CO)_4$	6.2×10^{-11}	1.4×10^{-10}	147.7	6.0	8.7
$Fe_2(C_5Me_5)_2(CO)_4$	2.5×10^{-11}	1.6×10^{-8}	165.0	4.2	4.1
$Rh_2(C_5Me_5)_2Cl_4$	1.5×10^{-11}	6.6×10^{-11}	133.5	51.9	57.0

Table IV. Solution ^{13}C-NMR Parameters of Cyclopentadienyl Carbons at 298 K for Species II–V

	9.4 T		6.3 T		
compd	T_1/s	η	T_1/s	η	τ^c/ps
$Rh(C_5Me_5)(CO)_2$	34.0	1.1	45.4	1.4	15
$Cr_2(C_5Me_5)_2(CO)_4$	21.6	0.9	30.1	1.3	21
$Fe_2(C_5Me_5)_2(CO)_4$	18.2	0.8	26.5	1.2	22
$Rh_2(C_5Me_5)_2Cl_4$	20.1	1.0	26.9	1.4	25

(24) Torchia, D. A. *J. Magn. Reson.* **1978**, *30*, 613.
(25) Torchia, D. A.; Szabo, A. *J. Magn. Reson.* **1982**, *49*, 107.
(26) Akasaka, K.; Ganapathy, S.; McDowell, C. A.; Naito, A. *J. Chem. Phys.* **1983**, *78*, 3567.

has been followed to determine $\Delta\sigma$ parameters from R_1^{CSA} values at two magnetic field strengths (6.3 and 9.4 T). These latter terms were simply determined by subtracting R_1^{DD} (determined from the measured NOE's) from the observed R_1 data; τ_c values used in these calculations were obtained from the dipolar term R_1^{DD} introducing a r_{C-CH_3} distance of 2.16 Å.

$\Delta\sigma$ parameters obtained by this procedure may be higher than their actual values because of the possible presence of other contributions to relaxation which are then included in R_1^{CSA}. However, as we have shown above, the introduction of these values in eq 5 led to a quite good agreement between calculated and experimentally measured T_1 for $^{13}C_{Cp}$ resonances in the solid state. Finally, it is worth noting that, for the system examined herein, the molecular motions occurring in the solid state are more efficient than those occurring in solution at providing more effective paths for the relaxation of ^{13}C resonances.

Conclusions

In this paper the reorientational motions occurring in some crystalline complexes containing C_5Me_5 ligands have been investigated by a combined use of "wide-line" and CP-MAS NMR spectroscopy and atom–atom potential energy barrier calculations. Two different processes have been detected, namely rotation of the methyl group about its C_3 axis and reorientation of the Cp ring about its C_5 coordination axis. In general, the activation energies obtained by ^1H spin–lattice relaxation time measurements compare well with the potential barriers calculated on the basis of the known crystal structures. However, contrary to what usually is observed for crystalline C_5H_5 derivatives,[5] the contribution of *intramolecular* origin can be substantial in permethylated complexes. In the cases of III and IV, in particular, the low activation energy found for the reorientation of the C_5Me_5 ligands has been explained on the basis of "synchronous" motions of the methyl groups during ring motion.

A similar correlation of intramolecular motions has been invoked to account for the reorientational motions of the C_6H_6 and C_2H_4 fragments in the polynuclear complex $Os_3(CO)_8(\eta^2\text{-}C_2H_4)(\mu_3\text{:}\eta^2\text{:}\eta^2\text{:}\eta^2\text{-}C_6H_6)$[27a] in accord with ^{13}C CP-MAS results.[27b]

In the case of II the activation energy is larger than PB_{tot} (22.0 vs 15.9 kJ·mol^{-1}; see Table I). This also applies to I, where the value of PB_{tot} (10.0 kJ·mol^{-1}) is smaller than the activation energies obtained from the analysis of the ^{13}C-CSA pattern (13.39 kJ·mol^{-1})[28] and by the ^1H spin–lattice relaxation time measurements discussed above (12.5 kJ·mol^{-1}). This is slightly disturbing since it is well-known that potential barrier calculations within the "static-environment" approximation tend to overestimate the barrier height.[12] It would appear that, at least in the case of I and II, this effect is overcompensated by the methyl/chlorine approximation adopted to account for free methyl rotation during ring reorientation. The difference between PB and E_a values could also be due to the contribution arising from metal-to-ligand bonding interactions. This contribution is neglected in potential barrier calculations. Therefore, in view of the different assumptions underlying the spectroscopic and theoretical analyses, only differences in order of magnitude between activation energies and potential barriers have to be regarded as significant.

We have also been able to show that ^1H "wide-line" and solution ^{13}C-T_1 NMR experiments can facilitate the comprehension of the ^{13}C-relaxation mechanisms operating in the solid state. It follows that the longitudinal relaxation rates of ^{13}C-atoms in rapidly reorienting π-bonded systems may be treated conveniently, as in the case of the solution.

In summary, while the NMR technique affords the actual quantitative information on the dynamic processess occurring in the solid state, the empirical calculations based on the structural data provide possible models for the reorientational process. We believe that the *cooperative* use of both approaches provides a better understanding of the intimate nature of the dynamic processes under investigation.

Experimental Section

Compounds I–V were prepared according to published methods.[29–31] The purity was checked by IR and NMR spectroscopy. The complete elimination of the solvent employed in the crystallization was obtained by sublimation and checked by observing the ^1H-NMR spectra of a concentrated solution of aliquots of the sublimated sample with $CDCl_3$ as solvent.

NMR measurements in solution were carried out on JEOL GSE 270 and on JEOL EX 400 spectrometers, where the ^{13}C nuclei resonate at 67.8 and 100.4 MHz, respectively. The samples for relaxation time measurements in solution were prepared by using Schlenk-tube techniques and oxygen-free $CDCl_3$ (20.30 mg of compound in 0.8 mL of solvent) and were degassed via the freeze–pump–thaw methodology. The nonselective inversion recovery pulse sequence was used to obtain T_1 values: the spin–lattice relaxation times were measured at 298 K, and a waiting time of more than $5T_1$ between the pulses was used. Nuclear Overhauser effects were measured by allowing a delay time of $10T_1$ between the pulses. Wide-line proton longitudinal relaxation times, T_1, were measured by the inversion recovery pulse sequence on a Stelar Spin-Master System operating at 60 MHz and on a JEOL GSE 270 spectrometer operating at 270 MHz. High-resolution solid-state ^{13}C NMR spectra were recorded at 67.8 MHz under conditions of ^1H–^{13}C cross polarization, high-power proton decoupling, the magic-angle spinning. Samples (typically 100–200 mg) were contained in rotors of zirconia and spun at spinning rates in the range 3.5–4.5 KHz. Chemical shifts (δ scale, high frequency positive) were referenced to external neat liquid tetramethylsilane (TMS). ^{13}C spin–lattice relaxation times in solids were measured by Torchia's method with a proton 90° pulse of 4 μs, carbon 90° pulse of 4 μs, and contact time of 3 ms. T_1 was calculated by means of a two-parameter nonlinear least-squares program by using at least 10 different τ values.

Acknowledgment. Financial support by the Ministero dell'Università e della Ricerca Scientifica e Tecnologica and by the Consiglio Nazionale delle Ricerche is acknowledged.

(27) (a) Braga, D.; Grepioni, F.; Johnson, B. F. G.; Lewis, J.; Martinelli, M. *J. Chem. Soc., Dalton Trans.* **1990**, 1847. (b) Heyes, S. J.; Gallop, M. A.; Johnson, B. F. G.; Lewis, J.; Dobson, C. M. *Inorg. Chem.* **1991**, *30*, 3850.
(28) Wemmer, D. E.; Ruben, D. J.; Pines, A. *J. Am. Chem. Soc.* **1981**, *103*, 28.
(29) Smart, J. C.; Robbins, J. L. *J. Am. Chem. Soc.* **1978**, *100*, 3936.
(30) Werner, H.; Klingert, B. *J. Organomet. Chem.* **1981**, *218*, 395.
(31) King, R. B.; Efraty, A. *J. Am. Chem. Soc.* **1972**, *94*, 3773.